FULL PAPER

Electron Density Investigation of a Push–Pull Ethylene (C$_{14}$H$_{24}$N$_2$O$_2$·H$_2$O) by X-ray Diffraction at T = 21 K

Alessandra Forni[a] and Riccardo Destro*[b]

Abstract: The electron charge distribution in a strongly twisted push–pull ethylene [PPE, 3-(1,3-diisopropyl-2-imidazolidinylidene)-2,4-pentanedione] has been determined by low temperature (T = 21 K) single-crystal X-ray diffraction analysis. The derived electronic properties are consistent with a zwitterionic molecule, as indicated by a charge transfer of 0.82(16) e from the *push* to the *pull* moieties and a charge polarization of 0.29(7) e on the olefinic bond. A dipole moment of 12(3) D has been determined, which compares well with ab initio theoretical results in terms of both modulus and orientation. The second moments, which have also been obtained with good precision, characterize PPE as a highly quadrupolar molecule. The special electronic features of the molecule confer particular topological properties to the electron density distribution, as evidenced by comparison with standard organic molecules. The crystallographic asymmetric unit of the present system includes one water molecule, which is hydrogen bonded to PPE. Its topological properties have also been investigated, together with an analysis of the hydrogen bonds involved.

Keywords: electron density distribution · push–pull ethylenes · strained molecules · topological analysis · X-ray diffraction

Introduction

Sterically overcrowded push–pull ethylenes have attracted attention for at least three decades, with regard to both their structural properties[1] and their possible applications in nonlinear optics.[2,3] Steric repulsion between the donor group(s) at one end of the olefinic bond and the acceptor group(s) at the other end results in a permanently twisted system, in which the central bond is elongated to a variable extent with respect to standard values.[4–12] In the solid state, intermolecular forces can also affect the molecular conformation, obscuring a simple correlation between the olefinic bond length and the twist angle. As this angle increases towards the perpendicular conformation, the molecule acquires a zwitterionic character, with the π electrons of the ethylenic C–C bond transferred to the acceptor group(s) and the positive charge localized on the donor group(s).

These structural peculiarities are associated with unusual properties of this class of compounds, such as high dipole moments and (hyper)polarizabilities,[2,8,9,13–15] low barriers to internal rotation about the ethylenic bond,[1,14–19] and strong intramolecular charge-transfer absorption bands.[20] On the whole, these properties make the push–pull ethylenes a useful class of NLO materials.[2] A possible means of acquiring further insight into these compounds is to derive and analyze the special features of their electron density (ED) distribution, from which several properties can be retrieved. Low temperature single-crystal X-ray diffraction has widely proved to be a powerful tool for obtaining accurate EDs, providing *quantitative* information about the nature of chemical bonds and the electrostatic properties of molecules.[21] To date, the main source of experimental information on charge delocalization in push–pull systems has been NMR spectroscopy.[16,22] In particular, the charge polarization of the formally double C–C bond can be derived from ^{13}C NMR spectra, the chemical shift difference of the two olefinic carbon atoms being a sensitive measure of double-bond polarization.[16] In this work, we present the results of a very low temperature X-ray charge density study on a push–pull ethylene, namely 3-(1,3-diisopropyl-2-imidazolidinylidene)-2,4-pentanedione monohydrate (PPE-H). Its

[a] Dr. A. Forni
CNR-ISTM, Istituto di Scienze e Tecnologie Molecolari
via Golgi 19, 20133 Milano (Italy)

[b] Prof. R. Destro
Dipartimento di Chimica Fisica ed Elettrochimica and CNR-ISTM,
Università degli Studi di Milano
via Golgi 19, 20133 Milano (Italy)
Fax: (+39) 02-50314300
E-mail: riccardo.destro@unimi.it

PPE
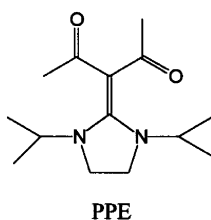
room-temperature X-ray crystal structure has already been reported, together with the results of ab initio STO-3G calculations on the non-optimized, experimental geometry of the isolated gas-phase molecule.[6] In that paper, hereinafter referred to as paper I, the structural features of PPE-H were thoroughly discussed, and the results of a topological analysis of the *theoretical* ED distribution were presented. In the present work, the *experimentally* derived ED is described and analyzed in terms of Bader's quantum theory of atoms in molecules (QTAM),[23] with particular emphasis on the region of the olefinic bond of PPE. Moreover, several charge density derived properties, such as the molecular electric moments and the charge transfer within the molecule, are presented and compared with ab initio computational results. Among them, we report a detailed analysis of the dipole moment and of its orientation with respect to both the molecular and crystallographic axes, quantities which are of great interest with regard to the macroscopic NLO properties of the crystal.[2] We emphasize the particularly low temperature of our experiment, 21(2) K, compared with most ED determinations by X-ray diffraction. At such a temperature, the atomic thermal motion is reduced to a minimum, allowing a more accurate description of ED and smaller experimental errors in the derived properties.

Results and Discussion

Structural analysis: Crystal data and the final results of the least-squares refinement are reported in Table 1. PPE-H crystallizes in the polar space group $Pna2_1$, which is one of the groups in which the conditions for non-vanishing macroscopic hyperpolarizability are satisfied. Molecules of PPE form infinite ribbons extending along the [010] direction, with the oxygen atoms of two different molecules hydrogen-bonded to a common water molecule (Figure 1). Molecules of adjacent ribbons interact through weak C–H···O bonds. A perspective view of PPE-H with the atom numbering scheme is shown in Figure 2.

Atomic fractional coordinates and anisotropic displacement parameters (ADPs, or thermal parameters) have been deposited with the CCDC (see Experimental Section). The 21 K root-mean-square amplitudes of vibration of the atoms with respect to their equilibrium position in the crystal, Δr_{rms}, are reported in Table 2. They are,

Table 1. Crystal data, details of data collection, and results of the refinement.

formula	$C_{14}H_{24}N_2O_2 \cdot H_2O$
M_r	270.4
space group	orthorhombic $Pna2_1$
Z	4
ρ_{calcd} [g cm^{-3}]	1.186
a [Å]	13.2511(23)
b [Å]	14.2055(21)
c [Å]	8.0429(14)
V [Å^3]	1513.98(43)
crystal dimensions [mm]	$0.30 \times 0.40 \times 0.55$
radiation	Mo$_{K\alpha}$
T (K)	21(2)
scan mode	$\omega/2\theta$
scan range [2θ, °]	$2.6 + S_{\alpha1-\alpha2}$ [a]
scan rate [2θ, ° min^{-1}]	3.0 [b]
$(\sin\theta/\lambda)_{max}$ [Å^{-1}]	1.15 [c]
h, k, l ranges	$-30 \rightarrow 30; -32 \rightarrow 32; -18 \rightarrow 0$
independent reflections	10066
reflections with $F^2 > 0$	9754
measured reflections	54710
exposure time [h]	1520
no. of observations	8511
no. of parameters	716
scale factor	1.0334(13)
extinction coefficient $\times 10^4$ [rad^2]	0.04(2)
$R(F), wR(F)$	0.0345, 0.0194
$R(F^2), wR(F^2)$	0.0305, 0.0367
goodness-of-fit	1.0881
max. Δ/σ	0.0005
for the data within the Cu sphere:	
$R(F), wR(F)$	0.0111, 0.0089
$R(F^2), wR(F^2)$	0.0107, 0.0171

[a] $S_{\alpha1-\alpha2}$ is the α_1, α_2 separation in the intensity profile. [b] A preliminary collection of the reflections with $2\theta > 55°$ was performed at variable rate in the range 3.0–8.0° min^{-1}. [c] Corresponding to $(2\theta)_{max} = 109.9°$ for Mo$_{K\alpha}$ radiation.

on average, just 36 % as large as those at room temperature, which were found in the range 0.179(1)–0.298(1) Å.[6] Such a reduction of the thermal motion, which is markedly larger than that observed for the amino acid α-glycine[24] on going from room temperature to 23 K, is a prerequisite for a reliable deconvolution of the ADPs from the static electron distribution.[25] As discussed in paper I,[6] together with a comparison with other push–pull ethylenes, steric hindrance causes the pentanedione group to be strongly twisted with respect to the imidazolidine ring. The dihedral angle between the least-squares plane through the seven non-H atoms of the first group and that through the five heavy

Table 2. Root-mean-square amplitudes of atomic vibration Δr_{rms} (Å) and normalized net atomic charges $q(e)$ for PPE-H.[30]

Atom	Δr_{rms}	q	Atom	Δr_{rms}	q
O1	0.0865(4)	−0.36(3)	C7	0.0784(5)	−0.11(6)
O2	0.0956(4)	−0.45(3)	C8	0.0774(5)	+0.05(6)
N1	0.0744(4)	−0.31(4)	C9	0.0770(5)	+0.09(6)
N2	0.0717(4)	−0.27(4)	C10	0.0931(5)	+0.01(6)
C1	0.0992(5)	−0.09(7)	C11	0.0939(5)	−0.04(7)
C2	0.0733(5)	0.00(4)	C12	0.0764(5)	+0.02(5)
C3	0.0706(5)	−0.19(5)	C13	0.0967(5)	+0.01(7)
C4	0.0765(5)	−0.07(4)	C14	0.1006(5)	−0.14(7)
C5	0.0970(5)	+0.11(7)	O3	0.1087(5)	−0.33(4)
C6	0.0666(5)	+0.10(6)	<H>[a]	0.1806	+0.08(5)

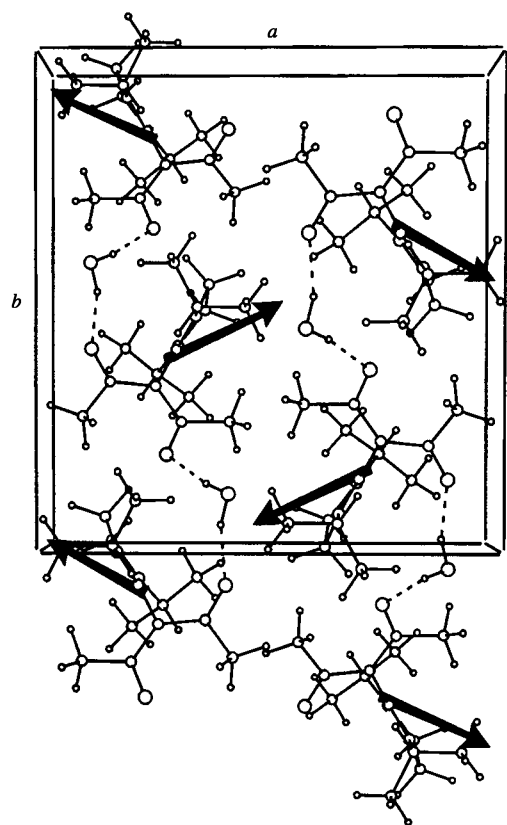[a] Weighted averages over the 26 H atoms of PPE-H.

Figure 1. Crystal packing view along *c* of PPE-H, the dipole moment direction of the PPE molecules being indicated. Dashed lines represent hydrogen bonding.
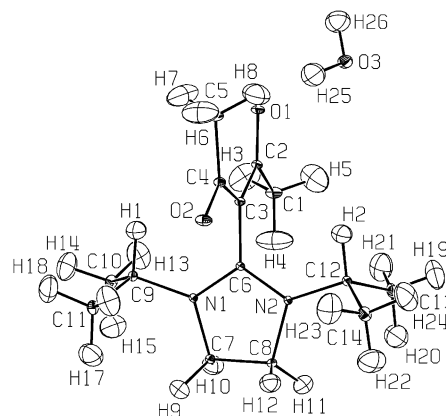

Figure 2. A view of PPE-H at 21 K with the atom numbering scheme. Ellipsoids are drawn at a 50% probability level.
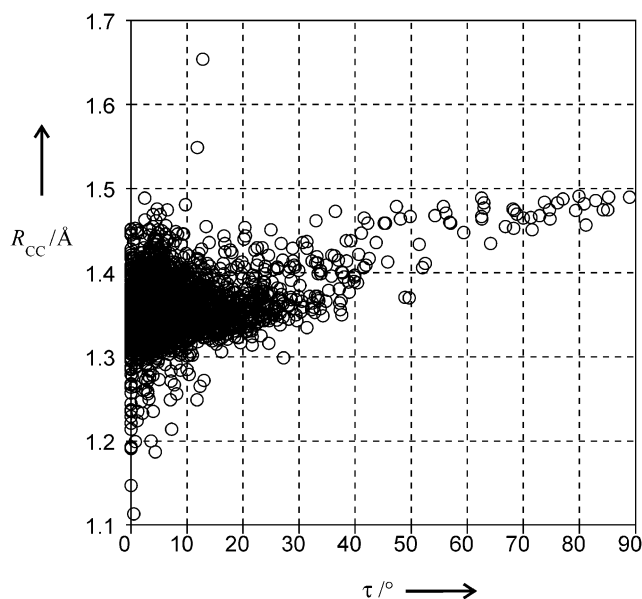

Figure 3. Distribution of the interatomic distances R_{CC} in tetrasubstituted ethylenes versus the dihedral angle τ (see text) for structures retrieved from the CSD.[26]

atoms of the latter measures 86.36(2)°, as compared with the room-temperature value of 85.0(1)°. To assess whether such a value is exceptionally large, a survey of the Cambridge Structural Database (CSD)[26] was performed, searching for compounds containing tetrasubstituted C=C fragments and getting information on both the consistency of twisted ethylenes in the database and their structural features. For each retrieved structure, two planes were computed and the dihedral angle τ between them stored, each of the planes being defined by one of the two ethylenic carbon atoms and by the two atoms bonded to it. A scattered yet clear correlation was found between the carbon–carbon distance R_{CC} and τ, as shown in Figure 3. The more strained ethylenes are strongly elongated with respect to the 1.331(9)–1.392(17) Å range found for $C_{sp2}=C_{sp2}$ bonds and approximate the unconjugated $(C=)C_{sp2}-C_{sp2}(=C)$ bond distance of 1.478(12) Å.[27] Of 3391 structures extracted, relatively few fragments fall in the region with large values of the dihedral angle τ and, among them, only three, apart from PPE-H, show a value of τ larger than 85°. Inspection of structures with $\tau \geq 50°$ reveals that, in almost all cases, they are push–pull 1,1-diaminoethylenes with the pull moiety consisting of NO_2, C=O or C=S groups.

The conformational strain of PPE also causes large deformations in the bonds adjacent to the olefinic one, particularly on the side of the pentanedione moiety. The formally single bonds C2–C3 and C3–C4 (1.4261(6) Å on average) undergo a significant shortening from the value of 1.464(18)

Å reported[27] for $(C=)C_{sp2}-C_{sp2}(=O)$ conjugated bonds, and the two C=O bonds (1.2536(7) Å on average) are very elongated with respect to the value for conjugated $(C=C-)C=O$ bonds, 1.222(10) Å. The average length of the two N–C6 bonds, 1.3308(10) Å, is slightly shorter than that reported for $(C=)C-N_{sp2}<$ bonds, 1.355(14) Å.[27]

All these values point to the ethylenic bond in PPE as being described as a single bond, with delocalization of the double bond charge on adjacent regions of the molecule. The implied charge transfer from the imidazolidine ring towards the pentanedione moiety, which, in principle, could range from being zero (biradical) to complete (zwitterionic species), will be discussed in a later section through evaluation of the atomic charges.

For a comprehensive discussion of the other structural features of PPE-H, we refer to paper I.[6] Here, we stress one of the advantages of working at very low temperature, that is a much better description of the H atoms. Refinement with polarized scattering factors for the H atoms[28]

yielded C–H bond lengths in good agreement with neutron diffraction values.[27] The average distance for the C–H bonds of the ring, 1.085(13) Å, is very close to the tabulated C_{sp3}–H (primary carbon) distance, 1.092(13) Å. The C9–H1 and C12–H2 bond lengths, 1.077(12) Å on average, are in agreement with the corresponding neutron value of 1.099(4) Å within two standard uncertainties (s.u.). Finally, the 18 C–H bond lengths in the methyl groups, ranging from 1.041(18) to 1.124(14) Å, are comparable with the neutron average value of 1.059(30) Å. In this connection, it was noted[29] that when only very low temperature neutron measurements are considered, larger methyl C–H distances are usually observed, approaching our average value.

Electrostatic properties: From the multipolar refinement, as described in the Experimental Section, the net charge q of each atom can be obtained as a sum over the monopole population and the nuclear charge of the atom itself.[30] The q values for PPE-H are reported in Table 2. Owing to the relatively large experimental errors associated with these quantities, comparison between atomic charges on different nuclei requires caution. However, the large negative charge on C3 (the largest on the whole set of C atoms), compared with the positive charge on C6, gives a reliable quantitative indication about the charge polarization of the ethylenic bond, since the resulting charge difference between these two atoms, 0.29(7) e, is certainly significant in terms of its standard uncertainty.

Even more reliable results can be gained by calculating cumulative charges on the relevant groups making up the molecule. A net charge of $-0.82(16)\,e$ is obtained on the pentanedione moiety, indicating a large degree of zwitterionic character for this push–pull ethylene. This value lies in the range of cumulative charges experimentally derived for the COO⁻ group of typically zwitterionic systems, such as the amino acids ʟ-alanine[31] and α-glycine[24] [$-0.59(2)\,e$ and $-0.97(3)\,e$, respectively]. Interestingly, the imidazolidine ring is virtually neutral, having a net charge of $-0.04(13)\,e$, while the positive contribution to satisfy the electroneutrality of the system is entirely due to the isopropyl groups, contributing $+0.54(14)\,e$ and $+0.32(15)\,e$ to the total molecular charge. For a comparison with the experimental X-ray atomic charges, RHF/6–31 G** and B3LYP/6–31 G** theoretical calculations on the isolated PPE molecule were also performed. A sum of the Mulliken populations associated with the atoms of each relevant group of the molecule gives $-0.71/-0.62\,e$, $+0.02/+0.09\,e$, and $+0.35/+0.26\,e$ for the pentanedione, the imidazolidine ring, and each isopropyl group, respectively, at the RHF/B3LYP level. These results agree well with the experimental group charges, fully confirming the large degree of charge transfer in PPE. The greater magnitude of the experimental charges on the more polarized groups, if compared in particular with the more reliable DFT results, is a well known consequence of the mutual polarization of the molecules in the crystal.[32]

The X-ray dipole and quadrupole moments of the molecule in the crystal were also computed, using the appropriate terms of the multipolar expansion.[33] The dipole vector has modulus $\mu = 12.0(29)$ D [or, in SI units, $40(9) \times 10^{-30}$

Cm], has its origin close to C6 (0.345 Å from it) when placed at the centre of mass of the molecule, and is oriented at 30(7)° with respect to the C3=C6 bond, towards the push moiety of the molecule (Figure 4). It lies approximately in the plane of the pentanedione, the angle between the dipole vector and the normal to the least-squares plane defined by the heavy atoms of this group being 76(11)°, and it makes an angle of 64(9)° with the normal to the least-squares plane through the imidazolidine ring. The angle between μ and the crystallographic [010] direction, along which the molecular ribbon develops, is 69(7)° (see Figure 1). The relatively
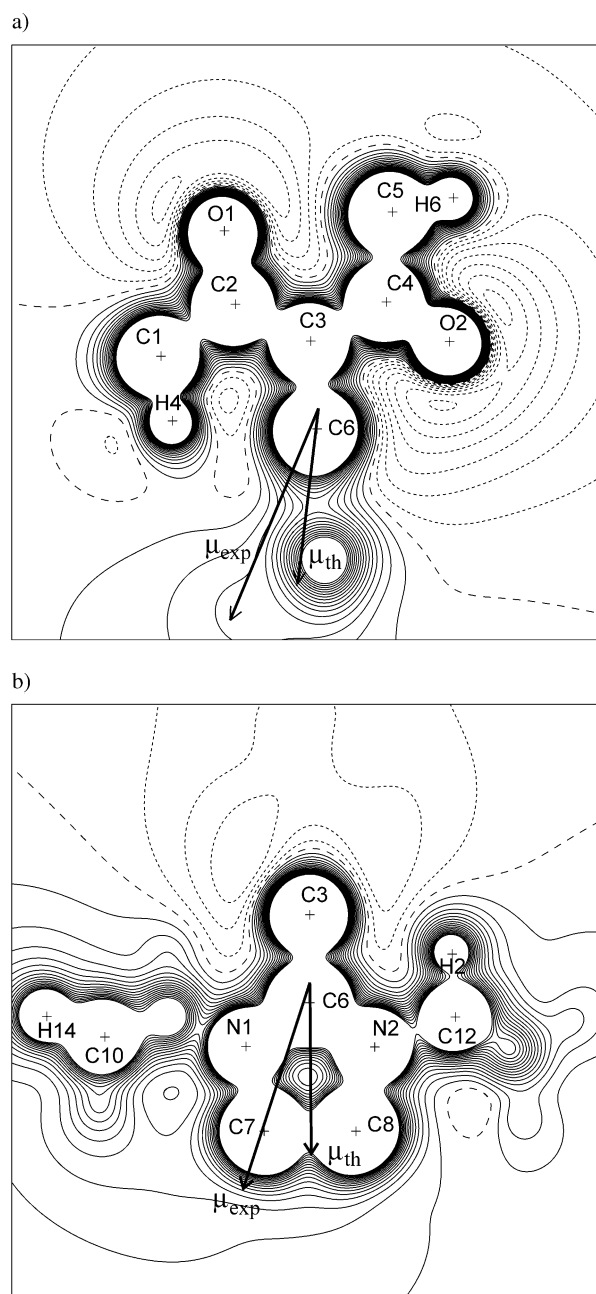

Figure 4. Electrostatic potential of PPE extracted from the crystal. Contour maps (10×10 Å) are shown in the planes defined by: a) the atoms C3, O2, O1, and b) the middle point of the C7–C8 bond and the atoms C8, C6. Contour intervals are 0.05 |e| Å⁻¹; solid lines positive, short dashed lines negative, long dashed lines zero contour. Atoms within 0.5 Å of the plane are labelled.

high magnitude of the dipole moment indicates a large separation of positive and negative charges in PPE. The theoretical RHF/B3LYP values, $\mu = 9.16/8.93$ D, lie approximately within the standard uncertainty of the experimental measurement but systematically below it, again in line with an increased polarization of the molecules in the crystal. The RHF/B3LYP dipole vectors are oriented at 12.6/10.7° with respect to the C3=C6 bond and make angles of 88.2/88.4° and 78.3/80.1° with the pentanedione and imidazolidine least-squares planes, respectively. All this indicates greater symmetry in the theoretical charge distribution with respect to the experimental one, which can clearly be explained in terms of the absence of any crystal effect on the former. By comparison of the experimental and theoretical components of $\boldsymbol{\mu}$ in the molecular inertial axes frame, $\mu_x = -1.1(36)$ versus 1.3/1.2 D, $\mu_y = 10.3(26)$ versus 8.8/8.6 D, $\mu_z = 6.2(17)$ versus 2.3/1.9 D, respectively, it can be seen that the only significant discrepancy, in terms of the experimental error, concerns the component along the z direction.[34]

The experimental second moments $\mu_{\alpha\beta}$ are reported in Table 3, together with the corresponding theoretical values. The traceless quadrupole moments, which can be obtained from the second moments by simple transformation,[21a] are reported in the Supporting Information. An analysis of the second moments obtained from X-ray diffraction experiments on a series of organic molecules[32] indicates that the $\mu_{\alpha\beta}$ values of PPE are comparable with those of typical highly quadrupolar molecules such as p-dicyanotetrafluorobenzene. The relatively low error in the diagonal components (16% in μ_{xx} and 4–5% in μ_{yy} and μ_{zz}) allows a meaningful comparison with theory. In all cases, they are underestimated with respect to theory, but the principal discrepancy concerns μ_{xx}, which is underestimated by almost 50%, while μ_{yy} and μ_{zz} are lower by only 10–20%. This indicates a significant contraction of the experimental charge distribution along a specific direction in the crystal, a feature that has also been observed in other crystal structures.[32]

Further information about the electrostatic properties of PPE can be derived from the electrostatic potential (EP).[35] A mapping of EP for the PPE molecule removed from the crystalline environment is shown in Figure 4, together with the experimental and theoretical (B3LYP/6–31G**) dipole moments. There is a clear separation between a negative region of EP, which is distributed around the oxygen atoms and the olefinic bond, and partially extends on the side of the imidazolidine ring facing the oxygen atom O2, and a

positive region localized in the plane of the ring and around the isopropyl groups. The asymmetric distribution of EP may specifically account for the significant deviation of the dipole moment from the imidazolidine ring. Figure 4a shows that the theoretical dipole is slightly displaced in the same direction as the experimental one.

Topology of the electron density: The relevant electronic properties of PPE were further elucidated by a topological analysis of the electron density $\rho(\mathbf{r})$. According to Bader's approach,[23] the nature of chemical bonds can be fully characterized by the properties of $\rho(\mathbf{r})$ at the bond critical points (bcps), that is, points at which the first derivatives of the ED vanish. Properties of intramolecular bcps in PPE and in the water molecule of hydration are reported in Table 4. A map of the negative Laplacian $-\nabla^2\rho(\mathbf{r})$ of PPE-H is reported in Figure 5.

For a bond A–B, the distances R_A, R_B from the critical point to each of the two bonded nuclei give information about the polarity of the bond itself.[36] For all the C–C bonds in PPE, the bcps are located approximately at the midpoint of the bond, as reflected by the R_A/R_{AB} ratios in Table 4, indicating a low or zero degree of polarity for these homonuclear bonds. Nevertheless, the greatest shift from the midpoint of the bond, equal to 7% of half the bond length R_{AB}, is observed for the C3=C6 bond, in agreement with the above discussed charge polarization of this bond. It might appear surprising that the bcp of this bond is shifted towards the more electronegative C3 atom, at variance with what is generally observed (see, for example, the C–H bonds in Table 4). However, a close inspection of the charge deformation around the two C atoms shows that along the bond there is a higher electron concentration in the proximity of atom C6 than close to atom C3. The map of the Laplacian of $\rho(\mathbf{r})$, shown in Figure 5a, neatly illustrates this point. It is noteworthy that topological analysis of the RHF/STO-3G theoretical charge distribution, as reported in paper I,[6] gave the same direction for the shift of the bcp along the C3=C6 bond, though a much larger shift, amounting to about 34% of half R_{AB}, was determined.

Table 4 also reports the values of the electron density and its Laplacian at the bcps (ρ_b and $\nabla^2\rho_b$, respectively), the eigenvalues λ_i of the matrix of the second derivatives of $\rho(\mathbf{r})$ or curvatures, which are related to the Laplacian by $\nabla^2\rho_b = \lambda_1 + \lambda_2 + \lambda_3$, and the bond ellipticity $\varepsilon = \lambda_1/\lambda_2 - 1$. The latter property gives a measure of the deviation of ρ_b from

Table 3. Second moments $\mu_{\alpha\beta}$ of PPE and water in PPE-H compared with theoretical results.[a]

Molecule	μ_{xx}	μ_{yy}	μ_{zz}	μ_{xy}	μ_{xz}	μ_{yz}
PPE						
exp[b]	−174(28)	−326(18)	−346(14)	−38(16)	−7(14)	26(12)
RHF/6–31G**	−326	−396	−403	0	−10	18
B3LYP/6–31G**	−318	−388	−396	−1	−10	15
water						
exp[b]	−12.9(10)	−17.6(8)	−19.4(6)	−0.3(8)	−0.2(7)	−0.4(6)
RHF/6–31G**	−13.3	−19.3	−24.0	0.0	0.0	0.0
B3LYP/6–31G**	−13.8	−19.5	−23.8	0.0	0.0	0.0
MP2/6–31G**	−13.8	−19.7	−26.6	0.0	0.0	0.0

[a] All quantities in SI units (i.e. $\mu_{\alpha\beta}/10^{-40}$ Cm^2). The results are given with respect to the inertial axes frame, with the center of mass chosen as the origin. For the water molecule, the major symmetry axis is y, and the molecule lies in the xy plane. [b] Present work.

Table 4. Bond lengths and one short intramolecular contact R_{AB} (Å), and properties of the corresponding bond critical points of the electron density: distance R_A (Å) of the bond critical point to atom A, electron density ρ_b (eÅ^{-3}), its Laplacian $\bigtriangledown^2\rho_b$ (eÅ^{-5}), curvatures λ_i (eÅ^{-5}), and bond ellipticities ε.

A–B	R_{AB}	R_A	R_A/R_{AB}	ρ_b	$\bigtriangledown^2\rho_b$	λ_1	λ_2	λ_3	ε
C1–C2	1.5179(6)	0.7273	0.48	1.75(3)	−12.2(7)	−12.8	−11.4	12.0	0.12
C2–C3	1.4240(6)	0.7148	0.50	2.15(3)	−18.4(8)	−17.5	−13.5	12.5	0.30
C4–C3	1.4282(5)	0.7378	0.52	2.13(3)	−18.0(7)	−16.7	−13.7	12.5	0.22
C5–C4	1.5095(7)	0.7401	0.49	1.72(3)	−11.7(7)	−12.4	−11.3	12.0	0.09
C3–C6	1.4725(7)	0.6872	0.47	1.85(3)	−13.7(8)	−13.2	−12.5	12.0	0.05
C7–C8	1.5312(10)	0.7965	0.52	1.61(3)	−9.2(7)	−10.6	−10.6	12.0	0.01
C9–C10	1.5259(8)	0.7691	0.50	1.70(3)	−10.8(7)	−11.9	−11.0	12.1	0.08
C9–C11	1.5306(8)	0.7675	0.50	1.68(3)	−10.6(7)	−11.8	−10.8	12.0	0.09
C12–C13	1.5294(7)	0.7792	0.51	1.70(3)	−9.7(6)	−11.5	−10.8	12.6	0.06
C12–C14	1.5282(7)	0.7994	0.52	1.71(3)	−10.7(7)	−11.9	−11.0	12.2	0.08
O1–C2	1.2539(6)	0.7893	0.63	2.80(5)	−35.7(26)	−27.0	−24.3	15.6	0.11
O2–C4	1.2533(7)	0.7823	0.62	2.85(5)	−35.2(24)	−26.2	−24.4	15.4	0.07
O1···C5	2.8398(6)	1.4282	0.50	0.058(6)	1.29(2)	−0.13	−0.08	1.51	0.53
N1–C6	1.3324(10)	0.7655	0.57	2.30(4)	−22.0(16)	−19.6	−15.6	13.3	0.26
N1–C7	1.4731(6)	0.8448	0.57	1.74(3)	−9.3(11)	−12.4	−10.8	14.0	0.15
N1–C9	1.4654(8)	0.8540	0.58	1.71(4)	−10.3(12)	−11.8	−11.3	12.8	0.04
N2–C6	1.3292(6)	0.7937	0.60	2.42(4)	−27.2(18)	−21.3	−16.7	10.8	0.28
N2–C8	1.4736(8)	0.8426	0.57	1.68(3)	−9.2(11)	−11.7	−11.1	13.6	0.06
N2–C12	1.4651(10)	0.8674	0.59	1.63(4)	−9.9(15)	−11.0	−10.1	11.2	0.09
C9–H1	1.066(11)	0.6545	0.61	1.93(5)	−18.6(19)	−18.0	−16.7	16.1	0.08
C12–H2	1.087(12)	0.6962	0.64	2.00(5)	−22.5(19)	−19.6	−19.3	16.3	0.02
C7–H9	1.076(13)	0.6864	0.64	2.01(5)	−22.5(18)	−19.9	−19.2	16.6	0.03
C7–H10	1.111(13)	0.7248	0.65	1.88(5)	−18.5(19)	−18.2	−17.7	17.3	0.03
C8–H11	1.077(13)	0.7076	0.66	2.05(5)	−23.1(21)	−21.0	−20.0	17.9	0.05
C8–H12	1.075(12)	0.6794	0.63	1.93(4)	−18.9(17)	−18.4	−17.6	17.1	0.04
$<$C–H$>_{meth}$[a]	1.084(21)	0.6622	0.61	1.88(7)	−17.1(23)	−17.1	−16.1	16.0	0.06
O3–H25	0.970	0.7245	0.75	2.63(8)	−41.2(49)	−41.4	−39.8	40.1	0.04
O3–H26	0.970	0.7297	0.75	2.56(7)	−36.0(45)	−39.9	−37.8	41.7	0.05

[a] Weighted averages over the 18 methyl C–H bonds.

axial symmetry, allowing quantification of the π character of covalent bonds.

The existence of a correlation between ρ_b values and bond lengths has been extensively investigated.[29,37,38] Generally, both experimental and theoretical data fit a simple linear model, $\rho_b = aR_{AB} + b$, very well, giving similar slopes and only slightly different intercepts depending on the method used to obtain the data. To reduce the systematic differences due to the methodological approach (experimental apparatus, data treatment, etc.), the properties of the CC bonds of PPE were compared with those of two organic molecules analyzed in our laboratory at $T < 25$ K, namely citrinin[29] and syn-1,6:8,13-bis-carbonyl[14]annulene (BCA).[39] Figure 6 shows the values of ρ_b versus R_{AB} for all three of these systems and the fitting curve obtained for citrinin ($a = -3.792$, $b = 7.418$).[40] On the basis of this fitting, three kinds of CC bonds were singled out for citrinin, that is, at increasing values of ρ_b: i) the single bonds not involved in the conjugation scheme, ii) the formally single, and iii) the double bonds of the conjugated system. The BCA values appear to agree with the fitting curve of citrinin.

Inspection of Figure 6 suggests that the olefinic C3=C6 bond ($R_{AB} = 1.4725$ Å) may be classified with good approximation as a conjugated single bond, though it should be considered extraneous to the conjugation scheme of PPE, owing to the perpendicular orientation of the two molecular moieties. The corresponding bond order, computed as $n = \exp\{A[\rho_b - B]\}$ with $A = 0.957$ and $B = 1.70$,[41] is $n = 1.15$, confirming the negligible double-bond character of the conjugated single bond. On the other hand, the low ellipticity of this bond, $\varepsilon = 0.05$, denotes its scarce π character,

making it more similar to non-conjugated single bonds. The largest deviations from the fitting curve relate to the C2–C3 and C3–C4 bonds ($R_{AB} = 1.4240$ and 1.4283 Å, respectively). While their lengths would characterize them as conjugated single bonds, very similar to the corresponding bonds of BCA, their ρ_b values approximate those of conjugated double bonds, indicating an acquisition of electron charge from the olefinic bond. The corresponding bond order, $n = 1.5$, is very close to the value, $n = 1.6$, assigned to benzene and obtained for the three conjugated double bonds of citrinin. The corresponding $\bigtriangledown^2\rho_b$ values (see Table 4) also compare well with the average value, $-17.6(9)$ eÅ^{-5}, obtained for the latter bonds. All the remaining C–C bonds fall in the region of the single bonds.

The topological properties of the two C=O bonds at the bcps make them more similar to the carboxylate bonds of some amino acids[31,42] than to a standard conjugated keto bond, for example, the C3=O13 bond of citrinin, confirming the zwitterionic nature of the present system. Indeed, the ρ_b values fall within the range 2.64–2.87 eÅ^{-3} reported for the former and are significantly larger than the value of 2.58(3) eÅ^{-3} obtained for the latter.

For the CN bonds, all the topological properties reported in Table 4 indicate a clear distinction between the two bonds to C6, which have a high degree of double-bond character, and the other two pairs of single C–N bonds. The difference is particularly evident in the Laplacian values and is due principally to the curvatures λ_1 and λ_2.

Finally, we mention the presence of a critical point along the line connecting O1 and C5, indicating a nonbonding interaction between these atoms. The physical meaning of this
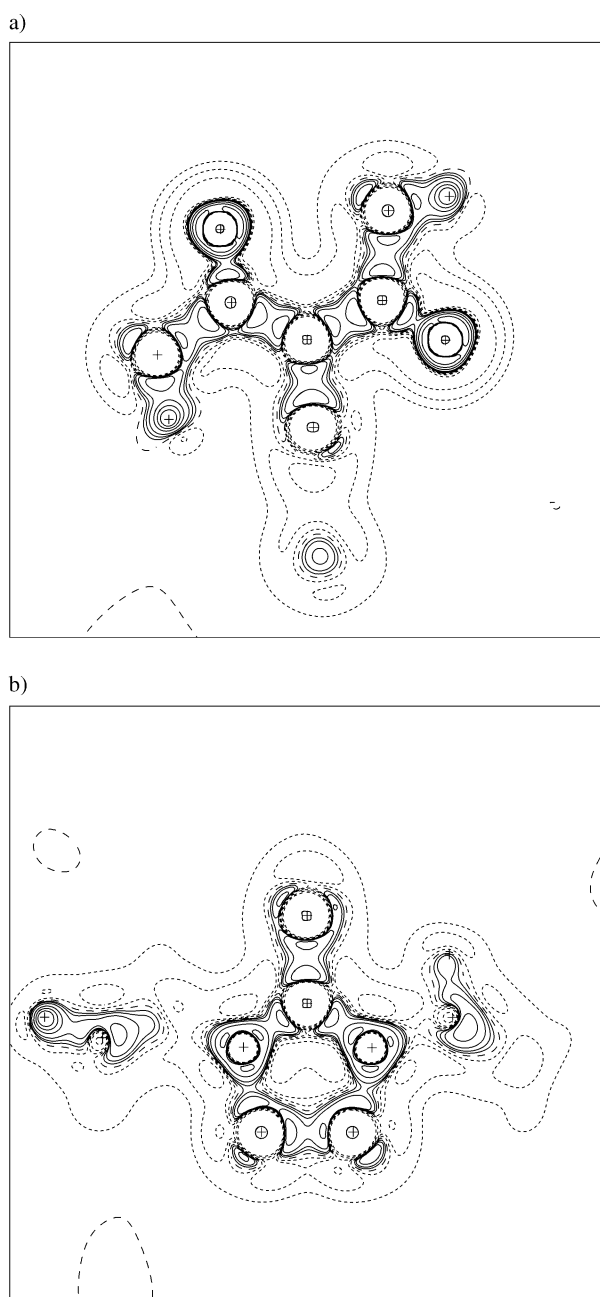
a)

b)

Figure 5. Maps (10×10 Å) of the negative Laplacian $-\nabla^2\rho$ of PPE-H in the same planes as in Figure 4. Contour lines are at 0, ± 2, ± 4, ± 8, ± 20, ± 40, $+80$ |e| Å^{-5}; solid lines describe the negative region of $\nabla^2\rho$ (indicating charge concentration), short dashed lines the positive region (indicating charge depletion).

critical point is under investigation, but we may note that: i) such a critical point is also found in the theoretical charge density, at both the RHF/6–31G** and B3LYP/6–31G** levels, with a ρ_b value of 0.084/0.089 eÅ^{-3}; and ii) the experimental value of 0.058(6) eÅ^{-3} for ρ_b is found not only for the molecule extracted from the crystal, but also when the surrounding molecules are included in the analysis.

Topological analysis was also employed to quantify the extension of the conjugated system in the molecule. From QTAM,[23,41] the eigenvector associated with the curvature λ_2 at a bcp determines the orientation of the plane in which
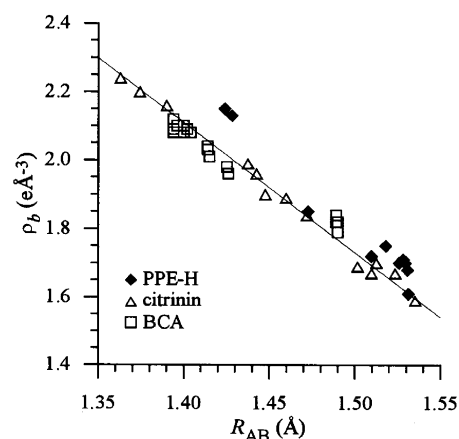

Figure 6. Electron density ρ_b at the CC bond critical points versus bond lengths R_{CC}. The values obtained for PPE-H (diamonds), citrinin[29] (triangles), and BCA[39] (squares) are reported. The fitting line to the citrinin values is also shown.

the electronic charge is preferentially accumulated along that bond, as occurs, for example, for a bond with π character. We computed, for each pair of contiguous bonds, the angle between the eigenvectors of λ_2 associated with the two bonds, small angles indicating an alignment of the π planes and hence conjugation between the bonds. The values of the angles in degrees are reported in Scheme 1, placed between the two bonds to which they refer. As expected, conjugation is totally lost along the olefinic bond C3=C6, as indicated by the large angles which the eigenvector of λ_2 at the bcp of C3=C6 forms with the corresponding eigenvectors of all the adjacent bonds. Two separate conjugation schemes are apparent in the molecule; one extends over the entire pentanedione moiety, where the eigenvectors are parallel to within 15°, while the other concerns the sequence C7-N1-C6-N2-C8, with a near optimal alignment around the atom C6. Finally, the large angles between the N–C bonds of the imidazolidine ring and the N–C bonds connecting the isopropyl groups to the ring exclude the possibility of hyperconjugative effects of the isopropyl groups with the conjugated system C7-N1-C6-N2-C8.

Intermolecular interactions: The topological properties describing the shortest intermolecular contacts of PPE with the water molecule and between adjacent PPE molecules are summarized in Table 5. The strongest interactions are clearly the O–H···O contacts, as indicated by the values of ρ_b. Owing to the large charges associated with the oxygen atoms of PPE, the hydrogen bonds that they form with water are relatively strong, as is apparent from a comparison
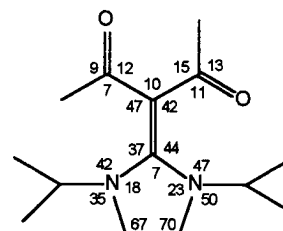
Scheme 1.

Table 5. Intermolecular A···H-D short contacts $R_{A···H}$ (Å) and properties of the corresponding critical points of the electron density: distance R_A (Å) of the critical point to atom A, electron density ρ_b (eÅ^{-3}), its Laplacian $\nabla^2\rho_b$ (eÅ^{-5}), curvatures λ_i (eÅ^{-5}), and bond ellipticities ε.

A···H–D	$R_{A···H}$	⊰A···H–D	R_A	$R_A/R_{A···H}$	ρ_b	$\nabla^2\rho_b$	λ_1	λ_2	λ_3	ε
O1[a]···H25–O3	1.90	170.8(10)	1.22	0.64	0.20(2)	1.4(5)	−1.54	−1.22	4.19	0.26
O2[b]···H26–O3	1.92	161.4(10)	1.24	0.65	0.16(2)	2.3(4)	−1.18	−0.74	4.27	0.59
O2[c]···H11–C8	2.23(1)	173.5(8)	1.32	0.59	0.11(1)	1.1(1)	−0.60	−0.49	2.20	0.22
O1[c]···H9–C7	2.35(1)	128.5(9)	1.36	0.58	0.09(1)	1.07(6)	−0.34	−0.33	1.74	0.03
O2[b]···H20–C13	2.36(1)	158.9(10)	1.48	0.63	0.04(1)	0.77(9)	−0.19	−0.15	1.11	0.27
O1[c]···H12–C8	2.44(1)	125.4(7)	1.37	0.56	0.08(1)	0.86(5)	−0.32	−0.30	1.48	0.07
O3 ···H10–C7	2.62(1)	125.0(7)	1.58	0.60	0.027(8)	0.60(3)	−0.10	−0.04	0.74	1.50
O3 ···H4–C1	2.72(1)	154.9(8)	1.52	0.56	0.048(6)	0.49(2)	−0.21	−0.18	0.88	0.17

[a] Symmetry code: $-x, -y, -1/2+z$. [b] Symmetry code: $-1/2+x, 1/2-y, z$. [c] Symmetry code: $1/2-x, 1/2+y, -1/2+z$.

with geometrical and topological values reported in the literature.[43] For the same reason, rather strong C–H···O interactions involving the O1 and O2 atoms are observed, while weaker interactions characterize the contacts of C–H groups with the water oxygen O3.

The water molecule in PPE-H: As discussed in the Experimental Section, the O–H distances are required to be elongated along their bond direction to the neutron value of 0.97 Å[44] in the course of the refinement. The bond angle H–O–H, 107(1)°, was instead coincident with the average neutron value reported by Chiari and Ferraris,[45] denoting a considerable improvement with respect to the room temperature value of 91(4)° reported in paper I.[6] For the water molecule, the measured dipole moment was $\mu = 2.5(2)$ D [$8.4(6)\times10^{-30}$ Cm]. This value is greater than the gas-phase microwave result, $\mu = 1.8546(4)$ D,[46] and the theoretical RHF/B3LYP/MP2 dipoles, 2.15/2.00/2.07 D. It is among the largest estimates of μ reported for water in organic crystals,[32] indicating a strong polarization for this molecule as well. The vector $\boldsymbol{\mu}$ makes an angle of 3(5)° with the bisector of the H–O–H angle and an angle of 88(5)° with the normal to the H$_2$O plane. These results are in close agreement with those obtained for the D$_2$O molecule in cytosine monohydrate,[47] and the negligible deviations from the twofold symmetry of an isolated H$_2$O molecule indicate, in our opinion, a reliable description of the experimental charge density for this molecule. The second moments for water are reported in Table 3. Similarly to what was observed for the PPE molecule, the experimental diagonal components are underestimated with respect to the theoretical values and a significant reduction, ranging from 18% (B3LYP) to 27% (MP2 result), is observed in only one component, μ_{zz}. In the other two directions, the second moments are reproduced by theory to within 10%.

Conclusion

The electron density distribution $\rho(\mathbf{r})$ of a push–pull ethylene (PPE) with a near-perpendicular arrangement of the olefinic moiety has been determined by very low temperature (21 K), high-resolution X-ray diffraction analysis. Detailed results have been obtained for some electrostatic properties of PPE, such as charge polarization and molecular electric moments, which were reproduced to a good approximation by accurate theoretical calculations. The molecule can be described as a zwitterion, with a relatively large degree of charge transfer from the diamino to the diketone groups. Large molecular dipole and quadrupole moments have been obtained, indicating a marked separation of the positive and negative charges, which are located principally on the isopropyl groups bonded to the diamine and on the oxygen atoms of the diketone, respectively. A topological analysis of $\rho(\mathbf{r})$ has revealed that the region of the ethylenic bond is characterized by unusual properties, as evidenced by comparison with standard organic molecules. The formally double bond shows features typical of a conjugated single bond, although the molecular conformation implies a low degree of conjugation between the donor and acceptor groups. The double-bond charge acquired by the pull moiety is delocalized over the carbonyls and over the two C–C bonds adjacent to the olefinic fragment. An unexpectedly large charge density has been found on the latter bonds, which cannot be simply related to their length. Other experimental electron density studies on organic molecules having atypical electronic features are planned to further investigate the presence of meaningful relationships between geometrical and topological properties.

Experimental Section

Data collection and processing: Details of the synthesis and sample preparation of the crystals of PPE-H are quoted in paper I.[6] A crystal, enclosed in a glass capillary to avoid loss of water of hydration, was mounted on a four-circle Syntex $P\bar{1}$ diffractometer equipped with a Samson closed-cycle helium cryostat.[48] In Table 1 we report the crystal data and some details of the data collection. Collected data were first corrected for decay, which was never greater than 2%, and then elaborated to include the intensity losses biasing high-order measurements, as a consequence of the finite range of the scan. To this end, an approximated approach to the method developed by Destro and Marsh,[49] which has been successfully applied to several other sets of data collected in our laboratory,[24,29,50] was followed. After correction for Lorentz and polarization effects, the intensity data were merged, giving $R_{int} = 7.22\%$ for all the data with $F^2>0$ and 5.21% for those with $F^2>2\sigma(F^2)$. On the other hand, R_{int} was 2.43% for the data with $\sin\vartheta/\lambda < 0.7$ Å^{-1}, indicating that only the high order reflections, which were particularly weak for the crystal under study, were affected by high experimental noise. In view of these considerations, we decided to class as observed, after merging, only those reflections with $F^2>2\sigma(F^2)$, for $\sin\vartheta/\lambda>0.65$ Å^{-1}, while retaining all the $F^2>0$ data with $\sin\vartheta/\lambda<0.65$ Å^{-1}. The structure refinement was then performed on this set of data.

Structure refinement: The collected intensities were interpreted with the aspherical atom formalism of Stewart,[25,51] as implemented in the Valray set of programs.[52] The electron density of an atom was modeled by a sum of two terms, a spherical part, describing both the inner core of the

atom and an unperturbed contribution to the valence, and an aspherical one, associated with the deformable valence. Both spherical contributions were taken to be equal to the Hartree–Fock atomic functions of Clementi,[53] and population parameters of the inner core were constrained to be equal for all the 19 non-H atoms. A radial scaling parameter κ for the unperturbed valences of C, N, and O was included in the refinement. The deformable part of the electron density was described by a multipolar expansion up to the octupole level for the C, N, and O atoms, and to the quadrupole level for the H atoms. Slater-type functions, $r^n \exp(-\alpha r)$, were used for the radial parts of the multipoles, where the power of r assumed the conventional values $n = 2, 2,$ and 3 for dipole, quadrupole, and octupole, respectively, on C, N, and O, and values of $n = 1$ and 2 for dipole and quadrupole on H. The α coefficients for C, N, and O were included in the refined set of parameters, with a common value for dipole, quadrupole, and octupole functions of each atomic species, while the standard coefficient for the H atoms, $\alpha = 2.48$ bohr^{-1}, was kept fixed during the refinement.[54] Final refined α values for C, N, and O were 3.04, 3.04, and 4.12 bohr^{-1}, respectively.

In addition to the multipole parameters, the conventional atomic and displacement parameters were refined for all atoms. For C, N, and O atoms, the usual least-squares procedure was followed, with the z coordinate of O1 fixing the origin. For H atoms, positional and isotropic displacement parameters U_{iso} were first refined, together with core populations, using the radial scattering factors. H atoms were then polarized in the direction of the atom to which they were bonded, using the curves of generalized scattering factors versus $\sin\theta/\lambda$ calculated for the H$_2$ molecule.[28] Afterwards, the positional parameters were kept fixed and the dipole terms, besides the U_{iso} values and the monopole terms, were refined. By this procedure, the lengths of the C–H and O–H bonds increased by about 0.1 Å, as usual, reaching acceptable values for the C–H distances (see Results section). As the O–H distances of the water molecule (0.892 and 0.901 Å) were still too short, these bonds were elongated along their direction to the neutron diffraction value (0.97 Å) observed for the water molecules in oxalic acid dihydrate.[44] Anisotropic displacement parameters (ADPs) for the H atoms were determined by a procedure developed in our laboratory,[55] based on the results of a rigid-body analysis[56] of the molecule and on spectroscopic information.[57] During the refinement, an extinction correction seemed necessary and an isotropic parameter for a type I crystal[58] with Lorentzian distribution of mosaicity[59] was included in the model (actually, the maximum extinction effect, for reflection 200, was an intensity decrease by less than 2%). The last cycles of minimization were computed with 716 variables, that is, besides extinction, 56 positional, 114 displacement, 6 radial, and 305 population parameters for the 19 non-H atoms, and 234 population parameters for the 26 H atoms. Each cycle gave an estimate of the scale factor k, which in Stewart's approach as implemented in Valray,[52] is not included in the least-squares parameters.

Refinement was based on the F^2 of the 8511 observed reflections, as defined at the end of the previous section, and with weights $w = 1/\sigma^2(F^2)$. Convergence was reached when $|\Delta\varepsilon|/\varepsilon < 10^{-6}$, where $\varepsilon = \Sigma w(F_o^2 - k^2 F_c^2)^2$ is the error function to be minimized and $\Delta\varepsilon$ is the variation of ε in two subsequent cycles. Full second derivatives were included in the last least-squares cycle to check the attainment of the true minimum and to correctly estimate the variances of the parameters.

Quality of data and of fit: Results of the refinement are summarized in Table 1. Acceptable values for the agreement factors R were obtained for the full set of data, but excellent values of all indices characterize the set of data within the Cu sphere. Owing to the high noise level in the experimental data beyond the Cu sphere, relatively high, still featureless residuals were obtained by calculating the density maps with $(F_o - F_c)$ Fourier coefficients on planes spaced by 0.01 fractional units, with a maximum value of 0.364 eÅ^{-3}. By truncating the Fourier sum to reflections with $\sin\theta/\lambda < 0.65$ Å^{-1}, the residuals decreased to below 0.087 eÅ^{-3}. The model was also tested for the deconvolution degree between thermal parameters and populations, by comparing the ADPs with those obtained on high order data with a refinement based on the IAM model, as calculated by SHELX.[60] The maximum difference in the principal components of the U tensor for the non-H atoms was of the order of four s.u.s, but on average the variations were within one s.u.

Molecular motions: The Hirshfeld rigid-bond test[61] on the U_{ij}'s of the non-H atoms gave a root-mean-square discrepancy between the mean-square displacement amplitudes of pairs of bonded atoms in the bond direction equal to 0.00048 Å^2, with a maximum difference of 0.00112 Å^2 for the pair N2–C12. A rigid-body TLS analysis[56] showed that the motions of the pentanedione group and of the imidazolidine ring are highly uncorrelated. A rather satisfactory fit to the observed U_{ij} values was obtained by analyzing the two moieties separately, the root-mean-square differences between observed and calculated values being $\Delta U_{rms} = 1.7$ s.u.$_{rms}(U_{obs})$ for the seven atoms of the pentanedione, and $\Delta U_{rms} = 1.5$ s.u.$_{rms}(U_{obs})$ for the five atoms of the ring plus the carbon atom C3. The corresponding corrections to the bond distances were in the range 0.0005–0.0019 Å, the smallest variation relating to the C3–C6 bond. In the Results and Discussion, the geometry uncorrected for thermal motion is considered throughout.

Cambridge Structural Database analysis: The CSD CONQUEST software (version 5.23, April 2002)[26] was used to search for structures containing C–C bonds with only two generic (no hydrogens) substituents for each carbon. This bond was specified to be either single or double and not to be part of a ring. For each retrieved fragment, the planes of each carbon atom and of its two bonded atoms were computed and the dihedral angle between them was stored. The VISTA software was used for graphical presentation of the data. The search was restricted to entries satisfying the following criteria: a) $R \leq 0.1$, b) error-free coordinates, c) no polymeric structures, and d) only organic compounds.

Computational details: RHF and DFT single-point calculations were performed on both PPE and the water molecule at the experimental geometry. For DFT calculations, the B3LYP functional was used.[62] MP2 calculations were also carried out on the water molecule. The program GAUSSIAN 98[63] was used throughout.

CCDC-208208 contains the supplementary crystallographic data for this paper. These data can be obtained free of charge via www.ccdc.cam.ac.uk/conts/retrieving.html (or from the Cambridge Crystallographic Data Centre, 12, Union Road, Cambridge CB21EZ, UK; fax: (+44) 1223-336-033; or deposit@ccdc.cam.ac.uk).

[1] a) J. Sandström, *Top. Stereochem.* **1983**, *14*, 83–181; b) I. Wennerbeck, J. Sandström, *Org. Magn. Reson.* **1972**, *4*, 783–789; c) J. Sandström, U. Sjöstrand, I. Wennerbeck, *J. Am. Chem. Soc.* **1977**, *99*, 4526–4527; d) J. Sandström, U. Sjöstrand, *Tetrahedron* **1978**, *34*, 371–378; e) R. Gompper, H.-U. Wagner, *Angew. Chem.* **1988**, *100*, 1492–1511; *Angew. Chem. Int. Ed. Engl.* **1988**, *27*, 1437–1455.

[2] J. F. Nicoud, R. J. Twieg, in *Nonlinear Optical Properties of Organic Molecules and Crystals* (Eds.: D. S. Chemla, J. Zyss), Academic Press, New York, **1987**, pp. 227–296.

[3] J. Fabian, R. Zaharadnik, *Angew. Chem.* **1989**, *101*, 693–710; *Angew. Chem. Int. Ed. Engl.* **1989**, *28*, 677–694.

[4] D. Adhikesavalu, K. Venkatesan, *Acta Crystallogr. Sect. C* **1983**, *39*, 1044–1048.

[5] J. Sandström, K. Stenvall, N. Sen, K. Venkatesan, *J. Chem. Soc. Perkin Trans. 2* **1985**, 1939–1942.

[6] R. Destro, U. Cosentino, G. Moro, E. Ortoleva, T. Pilati, *J. Mol. Struct.* **1989**, *212*, 97–111.

[7] a) K. Baum, S. S. Bigelow, N. V. Nguyen, T. G. Archibald, R. Gilardi, J. L. Filippen-Anderson, C. George, *J. Org. Chem.* **1992**, *57*, 235–241; b) K. Baum, N. V. Nguyen, R. Gilardi, J. L. Filippen-Anderson, C. George, *J. Org. Chem.* **1992**, *57*, 3026–3030.

[8] H. Osaka, T. Ishida, T. Nogami, R. Yamazaki, M. Yasui, F. Iwasaki, A. Mizoguchi, M. Kubata, T. Uemiya, A. Nishimura, *Bull. Chem. Soc. Jpn.* **1994**, *67*, 918–923.

[9] K. Mohanalingam, M. Nethaji, P. K. Das, *J. Mol. Struct.* **1996**, *378*, 177–188.

[10] U. Bemm, H. Östmark, *Acta Crystallogr. Sect. C* **1998**, *54*, 1997–1999.

[11] Z. R. Zhou, W. Xu, Y. Xia, Q. R. Wang, Z. B. Ding, M. Q. Chen, Z. Y. Hua, F. G. Tao, *Acta Crystallogr. Sect. C* **2001**, *57*, 471–472.

[12] P. V. Bernhardt, R. Koch, D. W. J. Moloney, M. Shtaiwi, C. Wentrup, *J. Chem. Soc. Perkin Trans. 2* **2002**, 515–523.

[13] G. Favini, A. Gamba, R. Todeschini, *J. Chem. Soc. Perkin Trans. 2* **1985**, 915–920.

[14] R. Benassi, C. Bertarini, E. Kleinpeter, F. Taddei, S. Thomas, *THEOCHEM* **2000**, *498*, 201–215.

[15] R. Benassi, C. Bertarini, L. Hilfert, G. Kempter, E. Kleinpeter, J. Spindler, F. Taddei, S. Thomas, *THEOCHEM* **2000**, *520*, 273–294.

[16] a) G. Fisher, W.-D. Rudorf, E. Kleinpeter, *Magn. Reson. Chem.* **1991**, *29*, 212–222; b) E. Kleinpeter, S. Thomas, G. Uhlig, W.-D. Rudorf, *Magn. Reson. Chem.* **1993**, *31*, 714–721.

[17] E. Kleinpeter, A. Koch, M. Heydenreich, S. K. Chatterjee, W.-D. Rudorf, *J. Mol. Struct.* **1995**, *356*, 25–33.

[18] R. Benassi, C. Bertarini, F. Taddei, E. Kleinpeter, *THEOCHEM* **2001**, *541*, 101–110.

[19] I. Alkorta, C. Wentrup, J. Elguero, *THEOCHEM* **2002**, *585*, 27–34.

[20] S. Inoue, Y. Aso, T. Otsubo, *Chem. Commun.* **1997**, 1105–1106.

[21] a) P. Coppens, *X-ray Charge Density and Chemical Bonding*, IUCr Texts on Crystallography, Oxford University Press, Oxford, **1997**; b) T. S. Koritsanszky, P. Coppens, *Chem. Rev.* **2001**, *101,* 1583–1627, and references therein.

[22] Y. Song, L. Spencer, W. B. Euler, W. Rosen, *Org. Lett.* **1999**, *1*, 561–564.

[23] R. F. W. Bader, *Atoms in Molecules: A Quantum Theory*, Oxford University Press, Oxford, **1990**.

[24] R. Destro, P. Roversi, M. Barzaghi, R. E. Marsh, *J. Phys. Chem. A* **2000**, *104*, 1047–1054.

[25] R. F. Stewart, *Acta Crystallogr. Sect. A* **1976**, *32*, 565–574.

[26] F. H. Allen, *Acta Crystallogr. Sect. B* **2002**, *58*, 380–388.

[27] F. H. Allen, O. Kennard, D. G. Watson, L. Brammer, A. G. Orpen, R. Taylor, *J. Chem. Soc. Perkin Trans. 2* **1987**, S1–S19.

[28] R. F. Stewart, J. J. Bentley, B. Goodman, *J. Chem. Phys.* **1975**, *63*, 3786–3793.

[29] P. Roversi, M. Barzaghi, F. Merati, R. Destro, *Can. J. Chem.* **1996**, *74*, 1145–1161.

[30] An excess of electron density of $0.066(44)e$ was obtained on the water molecule when summing the net charges on its atoms, and an equal and opposite charge was found on the PPE molecule. Since the observed charge transfer can be considered negligible in terms of experimental error, the net charges of each atom were normalized to give neutral molecules.

[31] R. Destro, R. E. Marsh, R. Bianchi, *J. Phys. Chem.* **1988**, *92*, 966–973.

[32] M. A. Spackman, *Chem. Rev.* **1992**, *92*, 1769–1797.

[33] M. Barzaghi, *PAMoC. Properties of Atoms and Molecules in Molecular Crystals* (version 01.01.2003), CNR-ISTM, Milano (Italy), **2003**.

[34] The y inertial axis extends almost in the direction of the C3=C6 bond, and the z axis lies approximately in the plane of the pentanedione group.

[35] a) R. F. Stewart, *God. Jugosl. Cent. Kristalogr.* **1982**, *17*, 1–24; b) R. F. Stewart, B. M. Craven, *Biophys. J.* **1993**, *65*, 998–1005.

[36] D. Cremer, E. Kraka, *Croat. Chem. Acta* **1984**, *57*, 1259–1281.

[37] R. F. W. Bader, T.-H. Tang, Y. Tal, F. Biegler-König, *J. Am. Chem. Soc.* **1982**, *104*, 946–952.

[38] a) P. R. Mallinson, K. Wozniak, C. C. Wilson, K. L. McCormack, D. S. Yufit, *J. Am. Chem. Soc.* **1999**, *121*, 4640–4646; b) A. Wagner, R. Flaig, D. Zobel, B. Dittrich, P. Bombicz, M. Strümpel, P. Luger, T. Koritsanszky, H.-G. Krane, *J. Phys. Chem. A* **2002**, *106*, 6581–6590.

[39] R. Destro, F. Merati, *Acta Crystallogr. Sect.B* **1995**, *51*, 559–570.

[40] In the previous work, the linear fit was calculated by using bond path lengths R_b instead of internuclear distances R_{AB}, but the two quantities were found to differ by less than 0.07% of the value of R_{AB} itself. In the present system, the maximum difference between the two distances is even smaller. Furthermore, the a and b values reported in the previous paper, where ρ_b and R_b were expressed in a.u., were −0.297 and 1.099, respectively.

[41] R. F. W. Bader, T. S. Slee, D. Cremer, E. Kraka, *J. Am. Chem. Soc.* **1983**, *105*, 5061–5068.

[42] P. Coppens, Y. Abramov, M. Carducci, B. Korjov, I. Novozhilova, C. Alhambra, M. R. Pressprich, *J. Am. Chem. Soc.* **1999**, *121*, 2585–2593.

[43] E. Espinosa, M. Souhassou, H. Lachekar, C. Lecomte, *Acta Crystallogr. Sect B* **1999**, *55*, 563–572.

[44] P. Coppens, J. Dam, S. Harkema, D. Feil, R. Feld, M. S. Lehmann, R. Goddard, C. Krüger, E. Hellner, H. Johansen, F. K. Larsen, T. F. Koetzle, R. K. McMullan, E. N. Maslen, E. D. Stevens, *Acta Crystallogr. Sect A* **1984**, *40*, 184–195.

[45] G. Chiari, G. Ferraris, *Acta Crystallogr. Sect. B* **1982**, *38*, 2331–2341.

[46] T. R. Dyke, J. S. Muenter, *J. Chem. Phys.* **1973**, *59*, 3125–3127.

[47] H.-P. Weber, B. M. Craven, *Acta Crystallogr. Sect. B* **1990**, *46*, 532–538.

[48] S. Samson, E. Goldish, C. J. Dick, *J. Appl. Crystallogr.* **1980**, *13*, 425–432.

[49] a) R. Destro, R. E. Marsh, *Acta Crystallogr. Sect. A* **1987**, *43*, 711–718; b) R. Destro, *Aust. J. Phys.* **1988**, *41*, 503–510; c) R. Destro, R. E. Marsh, *Acta Crystallogr. Sect. A* **1993**, *49*, 183–190.

[50] R. Soave, R. Destro, L. Belvisi, C. Scolastico, in *Electron, Spin and Momentum Densities and Chemical Reactivity* (Eds.: P. G. Mezey, B. E. Robertson), Kluwer Academic Publishers, Dordrecht, **2000**, pp. 275–283.

[51] R. F. Stewart, in *The Applications of Charge Density Research to Chemistry and Drug Design* (Eds.: G. A. Jeffrey, J. F. Piniella), Plenum Press, New York, **1991**, pp. 63–101.

[52] a) R. F. Stewart, M. A. Spackman, *VALRAY Users Manual*, Carnegie-Mellon University, Pittsburg, **1983**; b) R. F. Stewart, M. A. Spackman, C. Flensburg, *VALRAY Users Manual*, Carnegie-Mellon University, Pittsburg, and University of Copenhagen, Copenhagen, **2001**.

[53] E. Clementi, *IBM J. Res. Dev. IBM J. Res. Dev. (Suppl.)* **1965**, *9*.

[54] An α refinement of H atoms was also tested and the effects on the X–H bcps properties (X = C,O) were examined. Comparison of the model with unrefined α for H atoms showed a systematic shifting of the bcps towards the X atom, when α was refined, albeit only of the order of the s.u.s associated with the X–H bond lengths. The shortening of the X–bcp distances ranged from 0.012 to as much as 0.054 Å (0.027 Å on average) for the C–H bonds, and amounted to 0.052 and 0.036 Å for the two O–H bonds. Variations in ρ_b and $\nabla^2\rho_b$, on the other hand, were not significant in terms of their s.u. However, the Laplacian distribution around some H atoms assumed physically unrealistic features, suggesting that the model with unrefined α for the H atoms is preferable.

[55] P. Roversi, *Tesi di Laurea*, Università degli Studi di Milano, Milano, **1993**.

[56] V. Schomaker, K. N. Trueblood, *Acta Crystallogr. Sect. B* **1968**, *24*, 63–76.

[57] For the present system, spectroscopic data were derived from the RHF/6–31G* optimized geometry of PPE, ref. [63], which did not differ greatly from the experimental one. The computed frequencies were appropriately scaled by a factor 0.9 as suggested by several investigations (A. P. Scott, L. Radom, *J. Phys. Chem.* **1996**, *100*, 16 502, and references therein). Experimental frequencies for the water molecule were taken from the literature (J. Smets, A. Destexhe, L. Adamowicz, G. Maes, *J. Phys. Chem. B* **1997**, *101*, 6583). The ADPs of the H atoms were then introduced without further variation in the least-squares process, thereby allowing the quadrupole refinement of the H atoms. The validity of this approach can be judged by considering the differences between the equivalent U values computed from the H ADPs and the previously determined U_{iso} values. Such differences were always smaller than 2.7 s.u., and only 1.5 s.u. on average for all the H atoms.

[58] P. J. Becker, P. Coppens, *Acta Crystallogr. Sect. A* **1975**, *31*, 417–425.

[59] F. R. Thornley, R. J. Nelmes, *Acta Crystallogr. Sect. A* **1974**, *30*, 748–757.

[60] G. M. Sheldrick, SHELX-97. Program for the Refinement of Crystal Structures, University of Göttingen, Göttingen (Germany), **1997**.

[61] F. Hirshfeld, *Acta Crystallogr. Sect. A* **1976**, *32*, 239–244.

[62] a) C. Lee, W. Yang, R. G. Parr, *Phys. Rev. B* **1988**, *37*, 785–789; b) A. D. Becke, *J. Chem. Phys.* **1993**, *98*, 5648–5652.

[63] M. J. Frisch, G. W. Trucks, H. B. Schlegel, G. E. Scuseria, M. A. Robb, J. R. Cheeseman, V. G. Zakrzewski, J. A. Montgomery Jr., R. E. Stratmann, J. C. Burant, S. Dapprich, J. M. Millam, A. D. Daniels, K. N. Kudin, M. C. Strain, O. Farkas, J. Tomasi, V. Barone, M. Cossi, R. Cammi, B. Mennucci, C. Pomelli, C. Adamo, S. Clifford, J. Ochterski, G. A. Petersson, P. Y. Ayala, Q. Cui, K. Morokuma, D. K. Malick, A. D. Rabuck, K. Raghavachari, J. B. Foresman, J. Cioslowski, J. V. Ortiz, A. G. Baboul, B. B. Stefanov, G. Liu, A. Liashenko, P. Piskorz, I. Komaromi, R. Gomperts, R. L. Martin, D. J. Fox, T. Keith, M. A. Al-Laham, C. Y. Peng, A. Nanayakkara, M. Challacombe, P. M. W. Gill, B. Johnson, W. Chen, M. W. Wong, J. L. Andres, C. Gonzalez, M. Head-Gordon, E. S. Replogle, J. A. Pople, Gaussian 98, Revision A.9, Gaussian Inc., Pittsburgh, PA, **1998**.